JACS
JOURNAL OF THE AMERICAN CHEMICAL SOCIETY
Communication
pubs.acs.org/JACS

Isotropic High Field NMR Spectra of Li-Ion Battery Materials with Anisotropy >1 MHz

Ivan Hung,[†] Lina Zhou,[‡] Frédérique Pourpoint,[‡] Clare P. Grey,[‡] and Zhehong Gan*[,†]

[†]National High Magnetic Field Laboratory, Florida State University, Tallahassee, Florida 32310, United States
[‡]Department of Chemistry, University of Cambridge, Cambridge CB2 1EW, United Kingdom

Supporting Information

ABSTRACT: The use of a magic-angle turning and phase-adjusted spinning sideband NMR experiment to resolve and quantify the individual local environments in the high field ^{7}Li and ^{31}P NMR spectra of paramagnetic lithium-ion battery materials is demonstrated. The use of short radio frequency pulses provides an excitation bandwidth that is sufficient to cover shift anisotropy of >1 MHz in breadth, allowing isotropic and anisotropic components to be resolved.

Since the first rechargeable lithium-ion (Li-ion) battery was commercialized by Sony in 1991, the use of Li-ion batteries as power sources for portable electronic devices, such as laptops and cell phones, has grown dramatically. These batteries offer high volumetric and high gravimetric energy density and long cycle life. However, cost, safety, stored energy density, and charge and discharge rates as well as service life are issues that continue to plague the development of large-scale Li-ion batteries for electrical vehicles (EVs), plug-in hybrid electric vehicles (PHEVs), and stationary storage. New positive and negative electrodes have been developed during the past 30 years to address some of these issues,[1,2] and solid-state $^{6/7}$Li NMR has played an important role in characterizing these materials and monitoring the changes of the Li local (structural and electronic) environment during the charge and discharge processes.[3]

Many of the Li-ion electrode materials are paramagnetic either in their pristine or charged and discharged states. Because of the strong nucleus−electron spin dipolar interaction (giving rise to 'paramagnetic shift anisotropy'), magic-angle sample spinning (MAS) alone may not be sufficient to allow high-resolution NMR spectra to be obtained, in which the individual components are resolved. Spinning sidebands (ssbs) may overlap among themselves making isotropic shift assignment and quantitative analysis difficult especially for samples containing multiple Li sites, and/or broad and overlapping resonances. These problems are further intensified at higher B_0 magnetic fields as the electron−nuclear dipolar interaction scales linearly with field.[3] To alleviate this problem, low B_0 fields and ^{6}Li isotopic enrichment ($\gamma_{7Li}/\gamma_{6Li}$ = 2.6) are often used for reducing the broadening effects of paramagnetic shift anisotropy and, consequently, the width of the sideband manifolds in units of Hz. However, this comes at the cost of lower sensitivity and the need to enrich samples, particularly when they are extracted in the small quantities typically obtained from standard "coin cell" or "swagelok" batteries. Other nuclei, such as ^{31}P, ^{29}Si, and ^{11}B can be used as complementary probes, being particularly useful in investigating "charged" electrode materials, i.e., ones containing little or no Li. However, these nuclei (and ^{31}P in particular) have high gyromagnetic ratios and large hyperfine shifts due to the high covalency of the P−O (and Si−O and B−O) bonds,[4] making the use of very high spinning speeds and low fields essential for samples in which multiple sites are present.

In this communication, a NMR experiment that combines the magic-angle turning (MAT)[5] and the phase-adjusted sideband separation (PASS)[6] techniques to obtain isotropic NMR spectra with apparently infinite MAS spinning rates is presented. The experiment allows quantitative NMR spectra of paramagnetic electrode materials to be obtained without ssbs at the moderate and high B_0 fields available in most NMR laboratories. The MAT experiment was originally developed for separating the isotropic and anisotropic chemical shifts using very slow MAS. Recently, it has been shown that the broad bandwidth of $\pi/2$ (projection) pulses can cover the very large chemical shift anisotropy of some high-Z spin-half nuclei to obtain 'infinite speed' spectra under fast MAS.[7,8] On the other hand, PASS is an experiment consisting of a sequence of π-pulses applied at an array of predetermined timings under MAS. A Fourier transform of only a few t_1 increments separates the ssbs according to their order. The proposed experiment exploits the advantages of the highly efficient PASS and the exclusive use of short projection pulses from MAT to obtain isotropic NMR spectra at high magnetic fields (B_0 = 19.6 T, $\nu_0(^{1}H)$ = 830 MHz) from materials with shift anisotropy exceeding 1 MHz.

Figure 1a shows the projection-MATPASS pulse sequence. The three evolution segments spaced 120° apart in rotor position completely average out the anisotropic shift regardless of the spinning rate. Note that the third evolution segment, necessary to satisfy this condition, is included during the null evolution (p = 0) period enclosed by dashed lines, which is equivalent to a superposition of p = +1 and −1 evolution. The isotropic shift is refocused at the end of t_1 because the first two $t_1/3$ evolution periods (p = +1) have a total duration equal to the (p = −1) period prior to t_2 acquisition. The t_2 acquisition is shifted with t_1 such that the evolution period only encodes the anisotropic shift. This modification turns MAT into a PASS experiment, because the total t_1 evolution modulates the phase

Received: April 8, 2011
Published: January 10, 2012

dx.doi.org/10.1021/ja209600m | J. Am. Chem.Soc. 2012, 134, 1898−1901

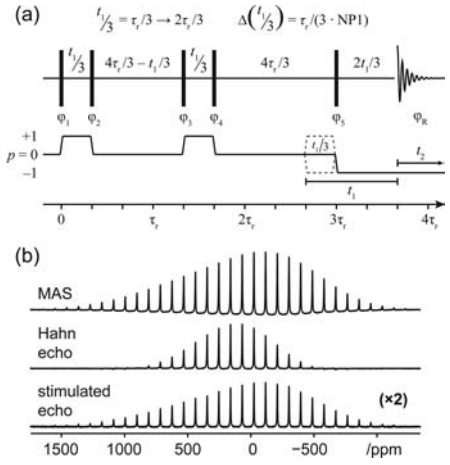

Figure 1. (a) Schematic of the projection-MATPASS experiment, where NP1 is number of t_1 values spanning one rotor period and black bars represent short pulses of equal length. A 20-step cogwheel[9] phase cycle determined using the program described in ref 10 selects the desired coherence transfer pathway: $\varphi_1 = 0$, $\varphi_2 = 12k\cdot(2\pi/20)$, $\varphi_3 = 10k\cdot(2\pi/20)$, $\varphi_4 = 2k\cdot(2\pi/20)$, $\varphi_5 = k\cdot(2\pi/20)$, and $\varphi_R = 5k\cdot(2\pi/20)$ with $k = 0, 1, 2, ..., 19$. (b) Comparison of ^{7}Li NMR spectra of $LiMnPO_4$ ($\nu_r = 30$, $\nu_1 = 132$ kHz) acquired with one-pulse excitation, rotor-synchronized Hahn echo and stimulated echo experiments to demonstrate the broader excitation bandwidth obtained by using 1.9 μs $\pi/2$ projection pulses rather than a standard π-pulse. All experiments were performed on a 19.6 T superconducting magnet with a Bruker DRX spectrometer and a home-built 1.8 mm MAS probe using a 100 ms recycle delay.

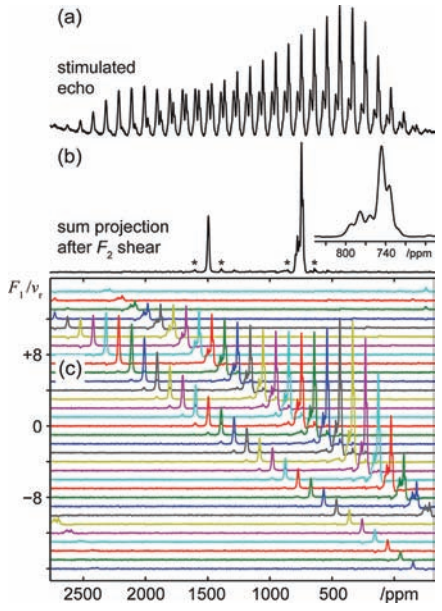

Figure 2. (a) ^{7}Li MAS spectrum of Li_2MnO_3 (prepared by heat treatment of Li_2CO_3 and Mn_2O_3 at 650 °C for 12 h, then at 850 °C for 24 h) sample.[15] (b) Isotropic spectrum obtained from summation of ssbs after shearing of (c) 2D MATPASS spectrum. Inset shows expanded view of the isotropic peaks around 760 ppm. Asterisks denote residual ssbs. Spectra were acquired at 19.6 T with $\nu_r = 33.3$ kHz, pulse widths of 1.0 μs, and NP1 = 32.

of the ssbs according to their order. Fourier transformation of t_1 then yields separated ssbs. In summary, the original MAT experiment,[5] which only employs small flip-angle ($\leq 90°$) pulses, is turned into a PASS experiment by a t_1-dependent delay of the acquisition time, as previously shown for the 5-π version of MAT.[11] Presented herein is the first instance of PASS spectra acquired solely using projection pulses.

It should be noted that the PASS separation requires a t_1 evolution spanning only one rotor period (τ_r) and does not have to start from $t_1 = 0$ as required in most 2D NMR experiments. This allows the first t_1 increment to be set to $t_1/3 = n\cdot\tau_r/3$ ($n \neq 3$), leaving sufficient time to accommodate for finite pulse lengths and radio frequency (rf) dead time without the need for a conventional spin echo. The pulse sequence is essentially a concatenation of two stimulated echo experiments and emphatically avoids the use of π-pulses, which can severely limit the excitation bandwidth, as shown by the spectra in Figure 1b of the positive electrode material $LiMnPO_4$. The use of only short pulses in the stimulated echo experiment provides a much broader excitation bandwidth than that obtained with a Hahn echo. However, the maximum intensity of the stimulated echo experiment is attenuated by a factor of 2 because only one component of the transverse magnetization is retained during the projection segment ($p = 0 \rightarrow +1 \rightarrow 0$). Thus, application of only short (small flip angle) pulses in projection-MATPASS also provides a much larger excitation bandwidth than previous techniques which incorporate one or more π-pulses, but the two projection segments yield a maximum signal of 25% compared to one-pulse excitation spectra. An alternative increase in excitation bandwidth can be obtained for paramagnetic systems via adiabatic frequency-swept pulses.[12]

Figure 2 shows the application of the projection-MATPASS experiment to Li_2MnO_3, chosen because it is a model sample for the class of paramagnetic battery materials with general composition xLi_2MnO_3-$yLi(Ni_{0.5}Mn_{0.5})O_2$. This sample has resonances with large shift anisotropy that span a breadth of more than 1 MHz resulting in numerous ssbs even at MAS frequencies greater than 30 kHz. The projection-MATPASS experiment yields a 2D spectrum with each of the ssbs separated into a different slice in F_1 (Figure 2c). A spectral shear[13,14] along F_2 aligns all the ssbs at the isotropic peak positions.[11] Subsequent addition of the F_1 slices yields a quantitative, purely isotropic spectrum as shown in Figure 2b. The observed isotropic ^{7}Li spectrum shows good agreement with a prior ^{6}Li MAS NMR spectrum ($\nu_r = 38$ kHz).[15] The single peak at ~1500 ppm corresponds to Li sites in the $[Li_{1/3}Mn_{2/3}]$ "honeycomb" layers of this material; the absence of other peaks at this position indicates that these layers are well-ordered. In contrast, the group of sites at ~760 ppm shows more than two peaks, which is inconsistent with what is expected from the crystal structure of this material. This phenomenon has been observed previously in low field ^{6}Li spectra and is ascribed to disorder in the *stacking* of the honeycomb layers (detailed discussion in ref 15.). The isotropic shifts observed in Figure 2 are collectively smaller by ~10 ppm than the prior ^{6}Li MAS NMR spectrum with $\nu_r = 38$ kHz due to the differences in sample temperatures that result from the heating effects of sample spinning. The temperature dependence of the hyperfine shift[16] complicates the use of the conventional method for identifying the isotropic resonances, which involves application of different spinning frequencies, because a variation of the spinning frequency also causes a change in sample temperature[17,18] and, thus, a shift of the whole spectrum. The MATPASS experiment yields isotropic peaks without this complication. Of particular relevance to the characterization of paramagnetic cathode materials, the results clearly demonstrate that the MATPASS experiment provides a

dx.doi.org/10.1021/ja209600m | J. Am. Chem.Soc. 2012, 134, 1898−1901

robust method for identifying and quantifying the concentration of the 1500 ppm resonance (i.e., the signature of Li in the transition-metal layers) in $x\mathrm{Li_2MnO_3}$-$y\mathrm{Li(Ni_{0.5}Mn_{0.5})O_2}$ and $x\mathrm{LiCoO_2}$-$y\mathrm{Li(Ni_{0.5}Mn_{0.5})O_2}$ (NMC) systems, an indicator of a class of defects in these materials, which has been strongly correlated with function.[3]

The robustness of the MATPASS approach is further demonstrated by its application to a cathode material with an associated ^{7}Li spectrum in which no individual isotropic resonances can be resolved (other than the resonance from Li in the diamagnetic fraction of the solid – an impurity) due to overlap of multiple broad resonances (Figure 3a). The sample

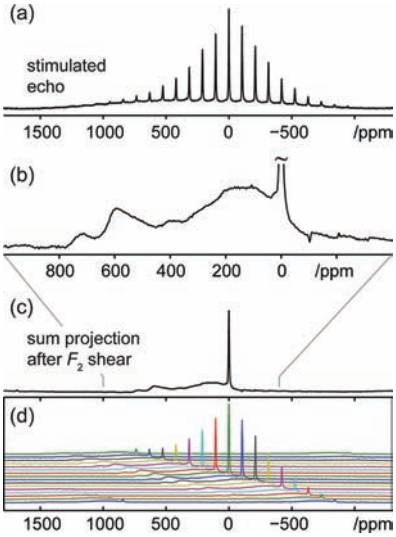

Figure 3. (a) ^{7}Li MAS spectrum of charged $\mathrm{Li_{2-x}FeSiO_4}$ following four charge–discharge cycles. (b) Expansion of resonances from 0 to 720 ppm from (c) isotropic spectrum of charged $\mathrm{Li_{2-x}FeSiO_4}$ obtained from summation of ssbs after F_2 shearing of (d) 2D MATPASS spectrum. Spectra were acquired at 19.6 T with ν_r = 34 kHz, pulse widths of 1.5 μs, and NP1 = 16.

has been extracted from a cell comprising the cathode material $\mathrm{Li_2FeSiO_4}$, following 4 charge cycles and a final charge to 3.7 V to yield a composition of approximately $\mathrm{LiFeSiO_4}$.[19] The MATPASS isotropic projection (Figure 3b,c) clearly demonstrates that the broad featureless resonance centered at ~300 ppm in Figure 3a is actually comprised of multiple isotropic resonances that spread over a range of about 800 ppm (>250 kHz). The resonances at 600–800 ppm are assigned to Li environments near Fe^{3+}, while the resonances at 200 ppm are environments that are observed during the transition of the material from its initial structure to the final more stable structure.

The ability of projection-MATPASS to yield isotropic MAS resonances for S = 1/2 nuclei with high gyromagnetic ratios and large hyperfine shifts, such as ^{31}P, is best illustrated by the ^{31}P spectra of $\mathrm{Li_3Fe_2(PO_4)_3}$ (Figure 4). The total breadth of the spectrum is approximately 1.2 MHz, requiring acquisition of the MAS spectrum in several parts due to limitations in the excitation bandwidth. Similarly, the 2D spectrum shown in Figure 4c was obtained by concatenation of two separate 2D spectra acquired using the carrier positions denoted by Tx1 and Tx2 in Figure 4b. The isotropic projections obtained from the 2D spectra are shown as red and blue dashed lines in Figure 4b. The cumulative projection (Figure 4b, black trace) shows three

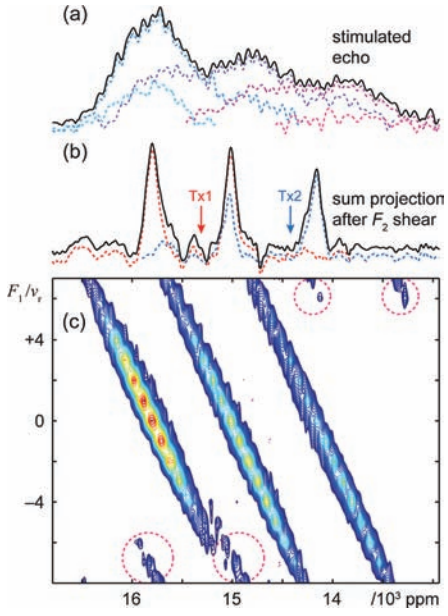

Figure 4. (a) ^{31}P NMR stimulated echo spectrum of $\mathrm{Li_3Fe_2(PO_4)_3}$ obtained by taking a skyline projection of several spectra acquired at carrier intervals of 300 kHz. (b) Isotropic projection obtained after shearing along F_2 of (c) 2D MATPASS spectrum. 2D MATPASS spectrum was acquired as two segments using carrier positions denoted by Tx1 and Tx2, ν_0 = 342.0 MHz, ν_r = 30 kHz, NP1 = 16, pulse widths of 1.5 μs, rf field amplitude of ν_1 = 125 kHz, and recycle delay of 30 ms; spectrometer and probe details are given in caption to Figure 1. Dashed circles enclose aliased spinning sidebands due to insufficient number of t_1 increments, NP1.

isotropic resonances with linewidths of 40, 43, and 51 kHz that exceed the MAS rate (and thus could not be resolved by MAS) and maxima at 14 160, 15 020, and 15 800 ppm, respectively. Notably, using the 2D MATPASS experiment at a single B_0 field and MAS frequency, this information is obtained straightforwardly, whereas multiple B_0 fields and MAS frequencies were previously necessary to resolve the interplay between the effects of sample heating and spinning sideband positions upon change of spinning speed, so isotropic resonances could be identified.[18] The straightforward acquisition of isotropic spectra using MATPASS should greatly facilitate the use of ^{31}P NMR as an additional probe for the characterization of phosphorus-containing Li-ion battery materials.

Several issues need be considered for the projection MATPASS experiment as applied to investigate Li environments in paramagnetic (Li-ion battery) materials. First, the ^{6}Li and ^{7}Li nuclides have spins S > 1/2 and possess electric quadrupolar moments. The first-order quadrupolar evolution can be refocused by MAT, just as chemical shift anisotropy, but only for coherences that remain in the same transitions (central or satellite) of the S > 1/2 spin. Coherences that switch transitions between the evolution segments are not refocused and can cause t_1 modulation of the signal intensity leading to residual ssbs. Simulations show that the intensities of residual ssbs remain less than 5% of the isotropic peak for C_Q values up to 200 kHz (Figure S1 in the Supporting Information). ^{7}Li has a relatively small quadrupolar moment, and most Li-ion battery materials have C_Q values within this limit.[20,21] Second, the projection-MATPASS pulse sequence is a nonconstant time experiment in contrast to the original PASS scheme;[6] hence,

dx.doi.org/10.1021/ja209600m | J. Am. Chem.Soc. 2012, 134, 1898–1901

the intensity of the t_1 slices is subjected to larger T_2 relaxation effects as the value of t_1 increases. This variation over the range of t_1 can also contribute to residual ssbs. The T_2 of these compounds are short, typically in the hundreds of microseconds,[22] but are still much longer than the rotor period at MAS frequencies greater than 30 kHz. Hence, relaxation effects are minimal as long as $T_2/\tau_r \gg 1$. Third, t_1 modulation of the projection pulse efficiency can also lead to residual ssbs. This modulation can become dramatic, as shown recently in the case of central transition spectra of half-integer quadrupolar nuclei, because of a level crossing mechanism.[23] MAT has an advantage over traditional PASS in that this modulation is averaged to zero in first order. For paramagnetic materials, the t_1 modulation due to the frequency offset of pulses can be significant, given that the shift anisotropy can span almost 10 times the magnitude of ν_1. As confirmed by the simulations in Figure S2, the frequency offset is the leading cause of residual ssbs observed experimentally. Thus, pulses with flip angles smaller than 90° should be used when necessary to ensure that the experiment has an adequately broad excitation bandwidth and acceptable residual ssbs, noting that increased excitation bandwidth comes at a cost of $(\sin\theta)/\sqrt{2}$ in the efficiency for each pulse, where θ is the on-resonance flip angle. Alternatively, since shift anisotropy scales linearly with field, the breadth of the spectra, and hence the stringent requirement on excitation bandwidth, can be reduced substantially by performing experiments at low B_0 fields. In this context, performing experiments at 19.6 T to give patterns with breadths in excess of 1 MHz may be considered a 'worst-case' scenario; presented primarily for demonstration purposes and to fully test the limitations of the proposed method.

It should be emphasized that the projection-MATPASS experiment excels in two aspects which have generally been mutually exclusive in previous high-resolution sideband separation methods: a broad excitation bandwidth and a low requirement in the number of t_1 increments. The broad excitation bandwidth obtained from exclusion of large flip-angle refocusing pulses makes the experiment viable for samples with large anisotropy (~1 MHz) and/or isotropic peaks far exceeding the MAS rate, both of which are by no means trivial cases. The evolution of only anisotropy in the indirect dimension allows the number of t_1 increments to be restricted to the minimum necessary without the need for methods such as States[24] or time-proportional phase incrementation,[25] significantly reducing the time−cost and complexity of the experiment. Furthermore, 2D sideband-separated spectra, such as those shown in Figures 2−4, can be obtained by direct 2D Fourier transformation of the acquired data *as is*, without any intricate manipulation.

In conclusion, a magic-angle turning sideband separation experiment that can be used effectively to obtain quantitative isotropic NMR spectra is presented here. Its application to Li-ion battery materials has demonstrated the capability to deal with large shift anisotropy in excess of 1 MHz and resonance lines broader than the MAS frequency, such as those found in paramagnetic systems with large electron−nuclear dipolar interactions. The experiment can be similarly applied to a wide range of other paramagnetic systems, from biology to materials chemistry (e.g., in catalytic systems or in metal organic frameworks).

■ ASSOCIATED CONTENT

Supporting Information

Simulation and comparison of residual sidebands. This material is available free of charge via the Internet at http://pubs.acs.org.

■ AUTHOR INFORMATION

Corresponding Author

gan@magnet.fsu.edu

■ ACKNOWLEDGMENTS

This work has been supported by the National High Magnetic Field Laboratory through cooperative agreement (DMR-0084173) with the NSF and the State of Florida. C.P.G. and L.Z. acknowledge support from the NECCES, funded by the U.S. DOE, BES under award no. DE-SC0001294. F.P. was supported by EPSRC and the Supergen consortium. Dr. Jongsik Kim is thanked for providing the sample of $Li_3Fe_2(PO_4)_3$. We thank Prof. P. Bruce and Dr. R. Amstrong (University of St. Andrews, U.K.) for providing the sample of $Li_{2-x}FeSiO_4$.

■ REFERENCES

(1) Whittingham, M. S. *Chem. Rev.* **2004**, *104*, 4271.
(2) Huggins, R. A. *Solid State Ionics* **2002**, *152*, 61.
(3) Grey, C. P.; Dupre, N. *Chem. Rev.* **2004**, *104*, 4493.
(4) Wilcke, S. L.; Lee, Y. J.; Cairns, E. J.; Reimer, J. A. *Appl. Magn. Reson.* **2007**, *32*, 547.
(5) Gan, Z. H. *J. Am. Chem. Soc.* **1992**, *114*, 8307.
(6) Antzutkin, O. N.; Shekar, S. C.; Levitt, M. H. *J. Magn. Reson., Ser. A* **1995**, *115*, 7.
(7) Hu, Y. Y.; Levin, E. M.; Schmidt-Rohr, K. *J. Am. Chem. Soc.* **2009**, *131*, 8390.
(8) Hu, Y. Y.; Schmidt-Rohr, K. *Solid State Nucl. Magn. Reson.* **2011**, *40*, 51.
(9) Levitt, M. H.; Madhu, P. K.; Hughes, C. E. *J. Magn. Reson.* **2002**, *155*, 300.
(10) Jerschow, A.; Kumar, R. *J. Magn. Reson.* **2003**, *160*, 59.
(11) Hung, I.; Gan, Z. H. *J. Magn. Reson.* **2010**, *204*, 150.
(12) Kervern, G.; Pintacuda, G.; Emsley, L. *Chem. Phys. Lett.* **2007**, *435*, 157.
(13) Massiot, D.; Touzo, B.; Trumeau, D.; Coutures, J. P.; Virlet, J.; Florian, P.; Grandinetti, P. J. *Solid State Nucl. Magn. Reson.* **1996**, *6*, 73.
(14) Hung, I.; Trebosc, J.; Hoatson, G. L.; Vold, R. L.; Amoureux, J. P.; Gan, Z. H. *J. Magn. Reson.* **2009**, *201*, 81.
(15) Breger, J.; Jiang, M.; Dupre, N.; Meng, Y. S.; Shao-Horn, Y.; Ceder, G.; Grey, C. P. *J. Solid State Chem.* **2005**, *178*, 2575.
(16) Tucker, M. C.; Doeff, M. M.; Richardson, T. J.; Finones, R.; Cairns, E. J.; Reimer, J. A. *J. Am. Chem. Soc.* **2002**, *124*, 3832.
(17) Grey, C. P.; Cheetham, A. K.; Dobson, C. M. *J. Magn. Reson., Ser. A* **1993**, *101*, 299.
(18) Kim, J.; Middlemiss, D. S.; Chernova, N. A.; Zhu, B. Y. X.; Masquelier, C.; Grey, C. P. *J. Am. Chem. Soc.* **2010**, *132*, 16825.
(19) Islam, M. S.; Armstrong, A. R.; Kuganathan, N.; Bruce, P. G. *J. Am. Chem. Soc.* **2011**, *133*, 13031.
(20) Ganapathy, S.; Rajamohanan, P. R.; Ganguly, P.; Venkatraman, T. N.; Kumar, A. *J. Phys. Chem. A* **2000**, *104*, 2007.
(21) Siegel, R.; Hirschinger, J.; Carlier, D.; Matar, S.; Menetrier, M.; Delmas, C. *J. Phys. Chem. B* **2001**, *105*, 4166.
(22) Tucker, M. C.; Doeff, M. M.; Richardson, T. J.; Finones, R.; Reimer, J. A.; Cairns, E. J. *Electrochem. Solid-State Lett.* **2002**, *5*, A95.
(23) Hung, I.; Gan, Z. H. *Chem. Phys. Lett.* **2010**, *496*, 162.
(24) States, D. J; Haberkorn, R. A.; Ruben, D. J. *J. Magn. Reson.* **1982**, *48*, 286.
(25) Marion, D.; Wuthrich, K. *Biochem. Biophys. Res. Commun.* **1983**, *113*, 967.